CHEMISTRY OF MATERIALS

pubs.acs.org/cm

Article

Ultrathin Hybrid SiAlCOH Dielectric Films through Ring-Opening Molecular Layer Deposition of Cyclic Tetrasiloxane

Kristina Ashurbekova,* Karina Ashurbekova, Iva Saric, Marco Gobbi, Evgeny Modin, Andrey Chuvilin, Mladen Petravic, Ilmutdin Abdulagatov, and Mato Knez*

Cite This: https://dx.doi.org/10.1021/acs.chemmater.0c04408

Read Online

ACCESS | Metrics & More | Article Recommendations | Supporting Information

ABSTRACT: Molecular layer deposition (MLD) is a powerful vapor phase approach for growing thin polymer films with molecular-level thickness control. We applied the ring-opening MLD process to deposit a siloxane-alumina hybrid organic−inorganic thin film using tetramethyl-tetravinylcyclotetrasiloxane (V_4D_4) and trimethylaluminum (TMA) as precursors. In situ studies of this process with a quartz crystal microbalance (QCM) showed a linear mass increase with the number of MLD cycles within a processing temperature window between 120 and 200 °C. The QCM study also revealed self-limiting surface chemistry. A growth per cycle of 1.4 and 1.6 Å and a density of 1.9 and 2.2 g cm^{-3} were determined by X-ray reflectivity (XRR) for the V_4D_4/TMA film deposited at 150 and 200 °C, respectively. X-ray photoelectron spectroscopy (XPS), attenuated total reflectance Fourier transform infrared spectroscopy (ATR-FTIR), and in situ QCM were employed to analyze the structural changes and composition of the film. High-resolution transmission electron microscopy (HRTEM) was used to confirm the conformality of the obtained coatings. The grown siloxane-alumina film, even as thin as 12 nm, showed an extremely low leakage current density (lower than 5.1×10^{-8} A cm^{-2} at ± 2.5 MV cm^{-1}), a dielectric constant (k) of 4.7, and a good thermal stability after one-hour annealing in air at 1100 °C. The obtained highly conformal and thermally stable siloxane-alumina insulating film can be used as a component of field-effect transistors, flash memories, and capacitors in modern electronic systems.

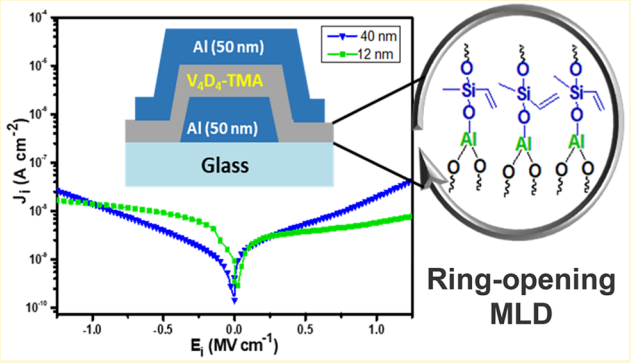

INTRODUCTION

Siloxane-based polymers possess a set of physical and chemical properties that are of great importance for many future application designs. The most interesting properties include a very high failure to strain and very low elastic moduli,[1] extreme hydrophobicity, thermal resistance, and chemical inertness,[2,3] just to name a few. These exceptional properties result from the highly flexible siloxane (Si−O−Si) backbone that imparts a high degree of molecular mobility and one of the lowest glass transition temperatures found among polymers (T_g < −100 °C).[4−6] These materials have found application as insulating layers in microelectronics,[7,8] pore sealings,[9] thin-film encapsulation layers,[10] antifouling coatings for membranes,[11,12] bioinert materials in biocompatible coatings,[13−15] and barriers.[16] The surfaces functionalized with patterned hydrophobic siloxane thin films have been utilized as templates for an ordered deposition of thin lamellar objects.[17]

Organosilicon polymers can also be converted into ceramic materials known as polymer-derived ceramics or PDCs.[18,19] This class of materials is capable of providing mechanical stability, corrosion protection, and heat dissipation at extremely high temperatures. High-temperature coatings are useful in various industries and are of utmost importance in the aerospace and automotive industries.[20−23]

Molecular layer deposition (MLD) is a gas-phase thin-film deposition technique for organic and hybrid organic−inorganic thin films that enables precise thickness and composition control.[24−26] The efficiency of the method has been demonstrated with the conformal deposition of ultrathin (<10 nm) and ultrasmooth (<1 nm RMS roughness) MLD coatings onto high aspect ratio and geometrically complex substrates.[27] By high-temperature pyrolysis of hybrid MLD films, one can synthesize a wide spectrum of conductive metal oxide-carbon composites or graphitic thin films.[28]

Atomic layer deposition (ALD)/MLD of SiO_2/siloxane-based materials are limited mainly by the poor reactivity of silicon precursors at low temperatures,[29] large reactant

Received: November 16, 2020
Revised: January 13, 2021

exposures,[30] corrosive byproducts,[31,32] or the need of a catalyst.[33] Initial attempts of Abdulagatov et al. to grow siloxane films using the sequential dosing of water with homo-bifunctional silane molecules, such as bis(dimethylamino)-dimethylsilane and 1,3-dichlorotetramethyldisiloxane, or hetero-bifunctional silane molecules, such as dimethylmethoxy-chlorosilane (DMMCS) and diisopropyl-isopropoxy-silane (DIPS), revealed that the growth rate became negligible after approximately 15 MLD cycles.[34,35] Abdulagatov et al. further used DMMCS and H_2O together with TMA in an ABCD process defined by TMA/H_2O/DMMCS/H_2O and DIPS together with TMA and H_2O in an ABC process with DIPS/H_2O/TMA sequence. The X-ray photoelectron spectroscopy (XPS) compositional analysis showed that both alumina−siloxane MLD films grown at 200 °C had a similar Si-to-Al ratio of 1:7. The authors explained the low atomic concentration of silicon in the films by the inefficient silane reaction with the hydroxylated surface.[35] Burton et al. reported that vinyltrimethoxysilane and trivinylmethoxysilane precursors are unable to remove completely the SiOH* surface species even at temperatures as high as 400°C.[29]

The ring-opening polymerization (ROP) of cyclic siloxanes is readily possible and is an example of a rare entropically driven polymerization. The vibrational and rotational freedom achievable in the linear siloxane units is much greater than that in the cyclic structures. In this work, we introduce cyclic siloxanes as a new class of silicon precursors for ROP MLD, uncommon from the first point of view because of the lack of reactive groups but reactive because of the ring nature of cyclosiloxane that enables to lower the MLD processing temperature.

We demonstrated earlier that a thin-film siloxane growth using a ROP reaction of vinyl cyclotrisiloxane (V_3D_3) and azasilane.[36] In the present work, MLD has been used to deposit siloxane-alumina hybrid organic−inorganic thin films using 2,4,6,8-tetramethyl-2,4,6,8-tetravinylcyclotetrasiloxane (V_4D_4) and trimethylaluminum (TMA). The growth was characterized in situ with a quartz crystal microbalance (QCM) and the grown thin films were characterized with various spectroscopies and microscopies to identify the growth mechanism. Furthermore, we show that the MLD process enables the formation of highly conformal, ultrathin films with excellent insulating properties, stability at high-temperature annealing conditions, and the possibility to control and vary the composition of the film with the processing temperature.

EXPERIMENTAL SECTION

The deposition of a thin film via MLD was performed in a custom made hot-wall-type reactor. Ultrahigh-purity nitrogen was used as a carrier gas. The deposition was performed under a constant nitrogen flow of 50 standard cubic centimeters per minute (sccm) and a reactor pressure of ∼1 Torr. 2,4,6,8-Tetramethyl-2,4,6,8-tetravinylcyclotetrasiloxane (V_4D_4) and trimethylaluminum (TMA) were purchased from Sigma-Aldrich and had purities of 98, and 97%, respectively. TMA was kept at room temperature during deposition, and 2,4,6,8-tetramethyl-2,4,6,8-tetravinylcyclotetrasiloxane (V_4D_4) was heated to 75 °C to provide sufficient vapor pressure. During the deposition, 6- and 2-second doses of V_4D_4 and TMA produced partial pressures of 0.30 and 0.25 Torr, respectively. The MLD experiments were carried out at reactor temperatures ranging from 120 to 200 °C, with the MLD cycle timing for the two-step process being 6/22/2/22 (in seconds), where 6 and 2 s are V_4D_4 and TMA dose times, respectively, and 22 s was the purge time.

High-resolution transmission electron microscopy (HRTEM) characterization was carried out with a FEI Titan 60−300 Cs-corrected microscope (Thermo Fisher, USA). To study the morphology of the deposited film on zirconia nanoparticles, the microscope was operated in a monochromatic mode at an accelerating voltage of 80 kV.

A thin cross-sectional sample of the film deposited on a silicon substrate has been prepared using FIB, involving the standard sample preparation protocol.[37] The TEM characterization and energy-dispersive X-ray spectroscopy (EDXS) (EDAX Octane, AMETEC, USA) mapping were done at an accelerating voltage of 300 kV.

In situ quartz crystal microbalance (QCM) measurements were performed using RC-cut, 6 MHz resonant frequency, polished, gold-plated, quartz crystal sensor (Phillip Tech.). The QCM crystal was mounted in a bakeable sensor housing (Inficon) and sealed using high-temperature epoxy (Epoxy Technology, USA). The QCM mass resolution was ∼0.3 ng cm^{-2}. The quartz crystal of the QCM was precoated with an ALD-grown, 60−80 Å thick Al_2O_3 film prior to any new measurement to generate identical conditions for all processes.

The thicknesses and densities of the samples were extracted from X-ray reflectivity (XRR) measurements with a PANalytical X'Pert Pro diffractometer with a Cu Kα radiation. Single-side polished P-type silicon (100) wafers were used as substrates for XRR measurements. The error bars obtained for MLD films grown on silicon wafers represent variations between three samples processed in the same experiment at different reactor positions.

Attenuated total reflectance Fourier transform infrared spectroscopy (ATR-FTIR) measurements were carried out with a PerkinElmer Frontier spectrometer. To increase the signal-to-noise ratio, pressed nanopowder of ZrO_2 (Sigma-Aldrich, particle size <100 nm) was used as a substrate for the ATR-FTIR measurements. All spectra were recorded in the range from 600 to 4000 cm^{-1} with 20 scans at 4 cm^{-1} resolution.

The chemical composition and bonding in the MLD films deposited onto a Si (100) substrate were examined by X-ray photoelectron spectroscopy (XPS) using a SPECS instrument, equipped with a hemispherical electron analyzer and a monochromatized source of Al Kα X-rays. The calibration of the energy scale in all XPS spectra was done by placing the binding energy of the characteristic C 1s peak at 284.5 eV. The XPS spectra were deconvoluted into several sets of mixed Gaussian−Lorentzian functions with Shirley background subtraction.

A CARBOLITE GERO laboratory high-temperature furnace was used for sample annealing. The ramp rate was 10 °C min^{-1}.

In metal/insulator/metal (MIM) device fabrication, the glass substrates were cleaned by ultrasonication with detergent dissolved in deionized (DI) water, acetone, and isopropanol (IPA). The cleaning procedure was performed in an ultrasonic bath for 20 min, with further drying in a stream of N_2. For MIM devices, 50 nm thick Al bottom and top electrode patterns were fabricated by UHV magnetron sputtering (AJA INT) with a base pressure of lower than 10^{-6} Torr through shadow masks with a deposition rate of 10 nm min^{-1}, and MLD films were deposited on top of the bottom Al electrodes before the deposition of the top Al electrodes. The widths of the top and bottom electrodes was 331 and 206 μm, respectively, leading to a junction area of 6.8 $\times 10^{-4}$ cm^2.

In electrical measurements, the electrical characterization and the capacitance measurement were performed in air using a Keithley 4200-SCS semiconductor analyzer connected to a variable temperature Lakeshore probe station.

RESULTS AND DISCUSSION

The proposed two-step MLD reaction of V_4D_4 and TMA for a siloxane-alumina hybrid film growth is schematically shown in Figure 1. This process is based on sequential surface reactions between V_4D_4 and TMA. During a steady-state growth, in step (A), V_4D_4 is exposed to an aluminum-methylated surface, where the formation of a four-centered intermediate promotes the V_4D_4 ring opening. As a result, a silicon-oxygen-aluminum

https://dx.doi.org/10.1021/acs.chemmater.0c04408
Chem. Mater. XXXX, XXX, XXX−XXX

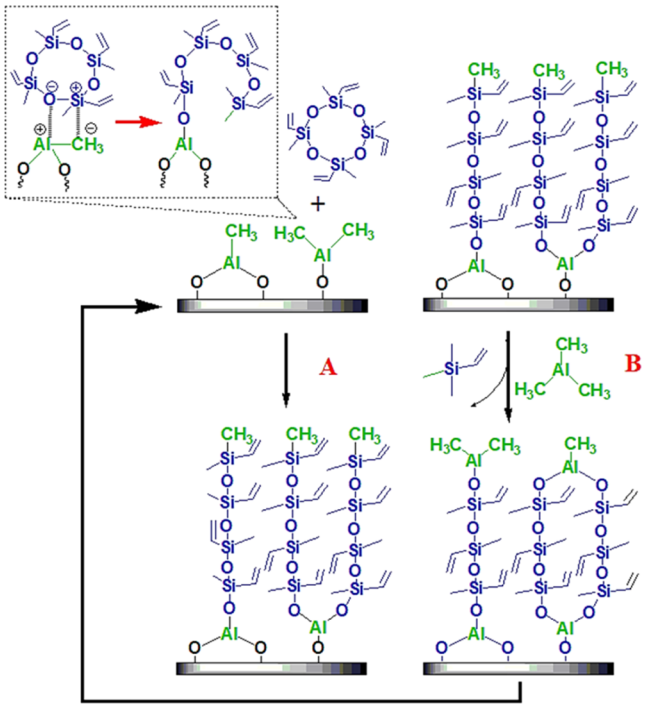

Figure 1. Proposed deposition scheme of the hybrid siloxane-alumina coating grown by MLD with V_4D_4 and trimethylaluminum (TMA) as precursors.

group is formed and the methyl ligand from aluminum is transferred to silicon.

The V_4D_4 ring opening polymerization (ROP) is an entropy-driven process due to the higher conformational freedom of the open polysiloxane chain in comparison to the cyclic siloxane.[38] The standard enthalpy of the V_4D_4 polymerization is nearly zero ($\Delta H_p^0 \approx 0$ kJ mol^{-1}) and the standard polymerization entropy is $\Delta S_p^0 = 6.7$ J mol^{-1} K^{-1}.[39] Thus, with $\Delta G_p < 0$, a polymerization is possible from the thermodynamic perspective.

In addition, the growth is amplified due to the 4 Si groups in one molecule, which theoretically allows a quadruple growth per cycle in comparison to the single Si atom containing the precursor. A further benefit is a circular shape, which increases the vapor pressure of the precursor in comparison to the linear counterpart and the entropy.

In step (B), TMA dosing leads to an electrophilic attack of the surface siloxane oxygen by Al, regenerating the aluminum-methylated surface. Vinyltrimethylsilane will be released as a byproduct.

One of the defining features of MLD is the self-limiting growth behavior that gives rise to two main characteristics like constant growth rate and saturative behavior.[40] The MLD type of growth of the siloxane-alumina films using V_4D_4 and TMA was examined in situ with QCM. The self-limiting behavior of the V_4D_4 and TMA surface reactions was studied at 150°C. The QCM results, showing a mass gain per cycle (MGPC) versus V_4D_4 and TMA dosing time, are shown in Figure 2a. The error bars obtained for each point represent the data spread from 40 data points (AB reaction cycles) for different experiments. The timing sequence used for the V_4D_4 saturation experiment was $X/22/2/22$ (V_4D_4 pulse/N_2 purge/TMA pulse/ N_2 purge) in seconds, where X stands for variable dosing time. In this experiment, the MGPC saturated at 17 ng

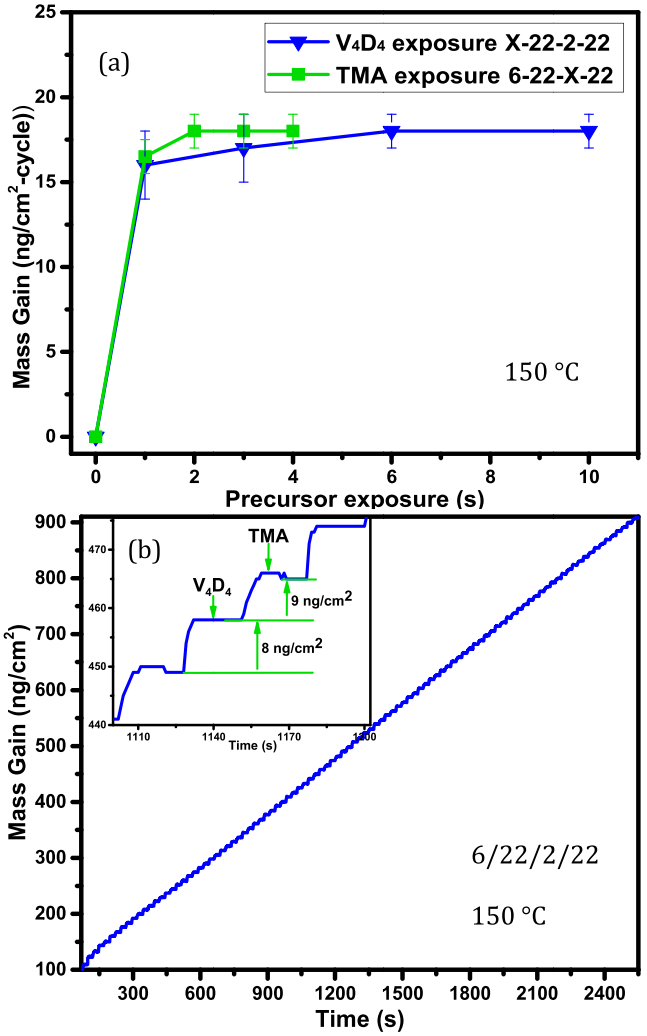

Figure 2. (a) QCM mass gain per cycle vs. V_4D_4 (black) or TMA (red) dosing time at 150°C. (b) QCM mass gain versus time during 50 MLD cycles at 150 °C. (b inset) Expanded view of a QCM signal during two MLD cycles.

cm^{-2} at 6 and 10 s dosing times of V_4D_4. The timing sequence for the TMA saturation experiments was $6/22/X/22$. After 2 seconds of dosing of TMA, the MGPC saturated at 17 ng cm^{-2}. Consequently, both surface reactions were found to be self-limiting. Purging times above 22 s did not alter the mass gain, neither after V_4D_4 nor after TMA pulses. Consequently, the timing sequence of 6/22/2/22 was used for all further experiments to fulfill a self-saturated condition for the studied MLD processes.

Figure 2b shows the QCM mass change vs. time during 50 cycles of V_4D_4 and TMA pulsing at 150 °C with alumina as a substrate. Alumina was predeposited by ALD at the same temperature to have a clean starting surface prior to MLD. A linear and reproducible mass increase was observed after the initial nucleation period of ~13 cycles. An expanded view of the QCM signal during two reaction cycles in a steady-state growth regime at 150 °C is presented in the inset of Figure 2b. Each precursor dose results in a mass increase. Upon dosing V_4D_4, we observed a mass gain of 8 ng cm^{-2}, and upon TMA dosing, a mass gain of 9 ng cm^{-2}, resulting in a total MGPC of 17 ng cm^{-2}.

https://dx.doi.org/10.1021/acs.chemmater.0c04408
Chem. Mater. XXXX, XXX, XXX−XXX

The temperature dependence of the MLD growth of V_4D_4/TMA was studied with QCM in a temperature range from 120 to 200 °C. Figure 3a demonstrates the MGPC dependence on the siloxane-alumina deposition temperature. A maximum growth rate of 24 ng cm^{-2} was observed at 180 °C. The contribution of V_4D_4 to the total mass gain decreased with increasing temperature. A maximum V_4D_4 mass gain of 9 ng cm^{-2} was observed at 120 °C, which decreased to 5 ng cm^{-2} at 200 °C. The opposite was observed for TMA. The TMA contribution to the total mass gain increased with the temperature. The mass gain during TMA dosing increased from 7 ng cm^{-2} at 120 °C to 15 ng cm^{-2} at 200 °C. Such a growth behavior makes the Si-to-Al ratio in the final film tunable simply by selecting the deposition temperature. No temperature 'window" with a constant MGPC was observed.

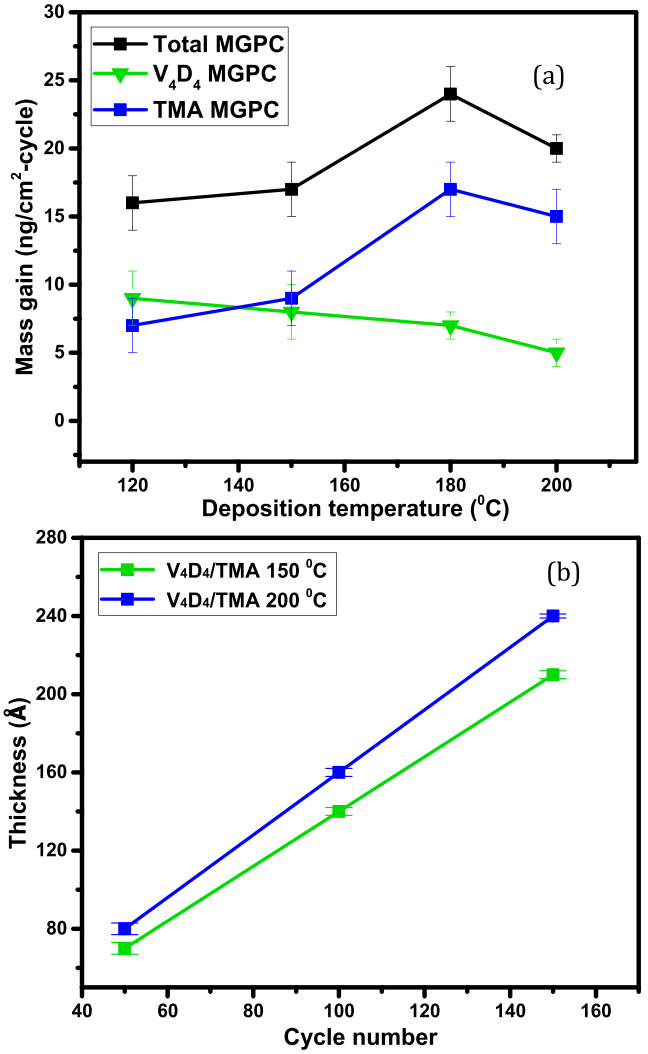

Figure 3. (a) QCM MGPC vs. deposition temperature. (b) XRR thickness versus MLD cycle number for the siloxane-alumina growth on Si(100) at 150 and 200 °C.

X-ray reflectivity (XRR) measurements were conducted to determine the growth rate, density and surface roughness, and the linearity of the thickness evolution of the film with the number of MLD cycles. The films were deposited on Si(100) wafers with a native oxide at 150 and 200 °C. The resulting thicknesses versus numbers of MLD cycles are presented in Figure 3b.

From the slope of the graph, a constant growth of 1.4 Å/cycle for the film deposited at 150 °C was deduced. The films had a density of 1.9 g cm^{-3} and an RMS roughness of 5.7 Å. The films grown at 200 °C showed a growth of ~1.6 Å/cycle. They had a density of 2.2 g cm^{-3} and an RMS roughness of 5.5 Å. The faster growth at 200 °C than at 150 °C is consistent with the QCM data. For comparison, ceramic ALD-deposited Al_2O_3 at similar process temperatures has densities around 3.0 g cm^{-3} and poly(dimethylsiloxane) (PDMS) has a density of 1.1 g cm^{-3}.[41,42] Our hybrid film approaches the densities of ceramic films, if deposited at higher temperatures, which is in agreement with the above-mentioned higher contribution of TMA to the hybrid at higher temperatures.

ATR-FTIR was performed to examine the bonding environment within the MLD film. The film was deposited onto pressed pills of ZrO_2 nanoparticles (NPs) to increase the surface area and thereby increase the signal-to-noise ratio. A spectrum of pure ZrO_2 NPs was recorded initially and used as a background spectrum for the sample spectra. Figure 4 shows the ATR-FTIR spectrum of a 40 nm thick MLD film, deposited at 200 °C, with vibrational features characteristic of organosilicon polymers. The bands between 2900 and 3100 cm^{-1} represent methyl (CH_3) and methylene (CH_2) stretching vibrations originating from saturated and unsaturated carbon in the film.

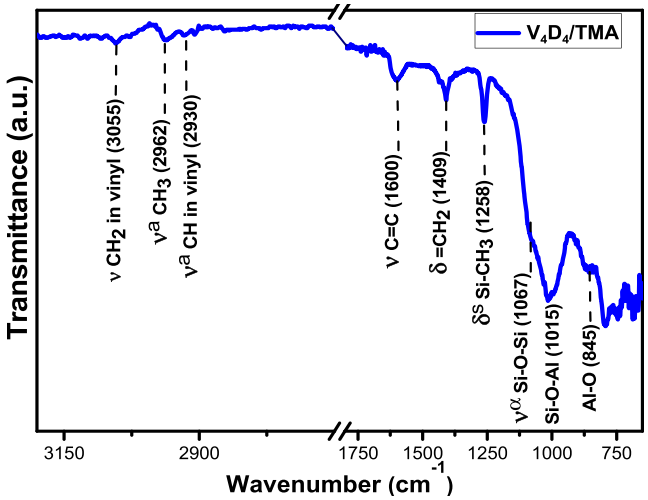

Figure 4. ATR-FTIR spectra of a 40 nm thick siloxane-alumina MLD film, deposited at 200 °C using a two-step V_4D_4/TMA process on pressed ZrO_2 particles.

Table 1S (in the Supporting Information (SI)) summarizes the wavenumbers of the peaks in Figure 4 and their assignment to the corresponding vibration modes. The strong Si−O−Al peak at 1015 cm^{-1} is consistent with a successful ring-opening reaction of V_4D_4 on the Al−Me surficial species. The shoulder around 1067 cm^{-1} indicates the absorption of the Si−O−Si chain. The lack of the characteristic absorption of cyclosiloxanes at 1000 cm^{-1} confirms the quantitative ring opening within the detection limit.[13] The peak at 845 cm^{-1} is attributed to Al−O moieties in the film. A closer look at the region between 1240 and 1300 cm^{-1} gives some more mechanistic insight.

https://dx.doi.org/10.1021/acs.chemmater.0c04408
Chem. Mater. XXXX, XXX, XXX−XXX

Namely, only one peak that indicates the degree of oxidation of the silicon atoms in the film is visible.[43] The band at 1258 cm^{-1} is attributed to the disubstituted silicon, which agrees with the proposed reaction mechanism, where the silicon in V_4D_4 contains a chain-building SiO_2MeVi unit. The spectrum also demonstrates features related to the vinyl groups on silicon, such as the $=CH_2$ bending at 1409 cm^{-1}, the C=C stretching at 1600 cm^{-1}, the asymmetric $=CH_2$ stretching at 3055 cm^{-1}, and the =CH stretching at 2930 cm^{-1}. All of the observed bands in the spectrum were expected from the proposed deposition scheme, thereby largely confirming the reaction mechanism.

High-resolution transmission electron microscopy (HRTEM) and energy-dispersive X-ray spectroscopy (EDXS) were used to examine the morphology and composition of the MLD films grown at 200 °C on a silicon substrate. A focused ion beam (FIB) technique has been involved to fabricate a thin cross-sectional sample for TEM measurements. Figure 5 shows a HRTEM image as well as the

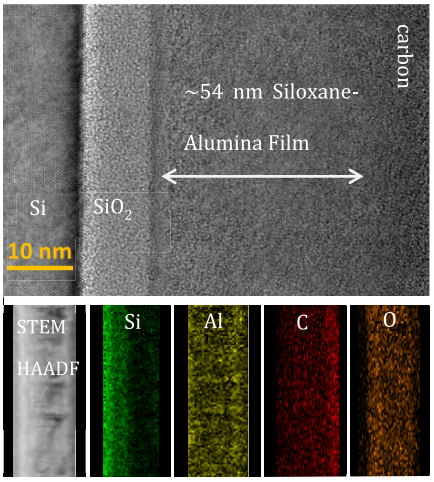

Figure 5. HRTEM imaging and EDXS elemental mapping data of a 54 nm thick siloxane-alumina film deposited on Si(100) with thermal SiO_2 at 200 °C.

EDXS elemental mapping of a 54 nm thick MLD film, deposited onto a silicon substrate with a 10 nm thick thermal silicon oxide layer. As expected, the siloxane-alumina film was amorphous. The growth of 1.6 Å/cycle, determined from the HRTEM micrograph, is in good agreement with the growth determined by XRR. The film composition and structure were further studied by elemental mapping with EDXS in the STEM mode, which confirmed the presence of Si, Al, C, and O in the film.

Figure 6 shows a series of XPS spectra around the C 1s, Si 2p, and Al 2p core-level regions of the 210 Å thick film deposited at 200 °C. The spectra were deconvoluted into sets of mixed Gaussian−Lorentzian functions with a Shirley background subtraction.[44] The C 1s spectrum in Figure 6a reveals several components originating from differently bound carbon within the siloxane-alumina MLD film. The C 1s spectrum was deconvoluted into three components, originating from Si−C=C, C−C/C−H, and O=C−O (surface contamination) bonds at binding energies (BEs) of 283.6, 284.5, and 288.4 eV, respectively. The Si 2p spectral region in Figure 6b is characterized by a single peak at 101.9 eV, assigned to the dioxygen-substituted (SiO_2C_2) bonding state of Si within the

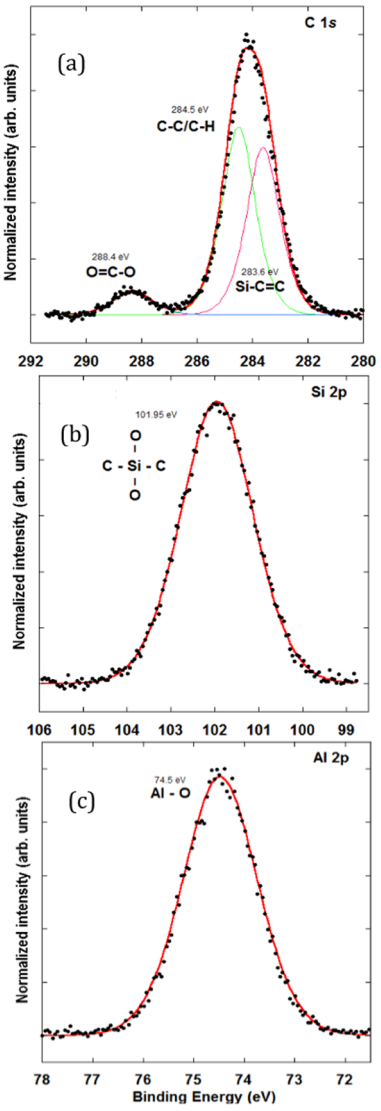

Figure 6. High-resolution XPS spectra of a 210 Å thick MLD film on Si(100) deposited at 200 °C: (a) C 1s, (b) Si 2p, and (c) Al 2p core levels.

film.[45] The spectrum around Al 2p in Figure 6c is also fitted by one dominant peak at 74.5 eV. From the reference data, typical binding energies for alumina Al 2p and silica Si 2p are 73.7[46] and 103.7 eV,[47] respectively. An increase in the BE of Al 2p from 73.7 eV to 74.5 eV, with a simultaneous decrease of the Si 2p BE from 103.7 eV to 101.9 eV, indicates the formation of the Al−O−Si bonds. Since Al is more electropositive than Si,[48] presence of Al−O units in the silica network decreases the BE of Si 2p and increases that of Al 2p.[49] In fact, the measured BEs are very close to the BEs of aluminosilicates,[50] further confirming the formation of the Al−O−Si bonds.

The overall composition and bonding environment of the components in the film were investigated by X-ray photoelectron spectroscopy (XPS). From the XPS survey scans of the films grown at 150 °C, the elemental composition ratio of 13:12:37:38 (in atom %) was determined for Si/Al/O:C. The ratio for the films grown at 200 °C was 11:19:38:32. With a Si-to-Al ratio of around 1:1 for the films grown at 150 °C and a ratio of around 1:1.7 for those grown at 200 °C, both films had a considerably lower Si-to-Al ratio than 4.5:1 as expected from the proposed reaction scheme. The ratios are consistent with

https://dx.doi.org/10.1021/acs.chemmater.0c04408
Chem. Mater. XXXX, XXX, XXX−XXX

the *in situ* QCM observations, where the V_4D_4-to-TMA mass gain ratio decrease from 150 to 200 °C. The ratio of Si to C was 1:3 for all deposition temperatures, correlating well with the proposed deposition scheme. This means that TMA cleaves the V_4D_4 molecule into −OSiMeVi− units, maintaining the original Si:C ratio of 1:3.

Based on the compositional analysis, the growth mechanism can be refined. Figure 7 schematically shows a plausible growth

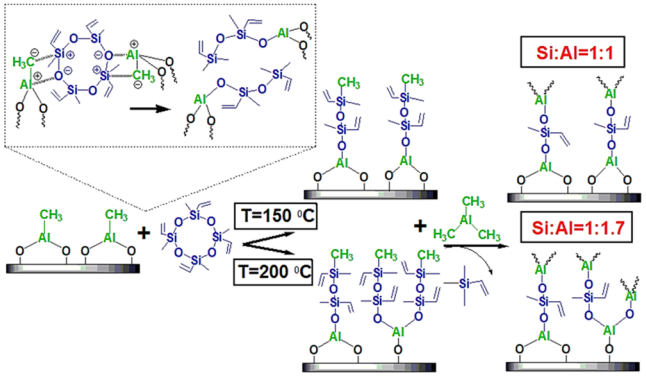

Figure 7. Mechanism of siloxane-alumina MLD using V_4D_4 and trimethylaluminum (TMA) at 150 and 200°C.

mechanism with V_4D_4 and TMA at 150 and 200 °C. The differing Si:Al ratios at the two processing temperatures suggest that one V_4D_4 molecule reacts with more than one Al-CH_3 surface site, potentially splitting V_4D_4 into more parts, as shown in the inset of Figure 7. This degradation reaction of V_4D_4 becomes more pronounced with increasing temperature, resulting in an aluminum oxide-like film growth. This could be due to an increase in the number of substitution reactions at 200 °C, as shown in Figure 7.

In principle, as an alternative to the reaction of V_4D_4 and TMA, precursors such as diethoxy(methyl)vinylsilane with TMA and similar could be used for a siloxane-alumina deposition. Given the various reported processes mentioned in the Introduction, we foresee an MLD reaction mechanism for diethoxy(methyl)vinylsilane and TMA as depicted in Figure 1S (in the SI). A siloxane-alumina MLD process with the above-mentioned precursors would either result in growth termination or in alumina-like films with the highest possible theoretical Si-to-Al ratio of 1:2 (page 2, SI), in agreement with earlier studies that showed that the experimental Si-to-Al ratio is much lower than the theoretical prediction.[35] Especially the expected partial termination of the film growth upon the use of diethoxy(methyl)vinylsilane in comparison to the here observed linear growth of the film makes the use of cyclic siloxanes very valuable and versatile with regard to the final film composition.

High-resolution TEM imaging was used to examine the conformality of the siloxane-alumina thin film. Figure 8a shows a TEM image of ZrO_2 NPs coated with a 50 Å thick MLD film obtained from the V_4D_4/TMA process at 200 °C. ZrO_2 NPs were chosen for their high surface area and good contrast versus that of the deposited film. The micrograph in Figure 8a shows the conformally coated NPs, confirming a successful MLD process. HRTEM images at higher magnification show the amorphous structure of the MLD film (Figure 8b).

Figure 2S (in the SI) shows the thickness changes in the siloxane-alumina films after one-hour annealing in air at various

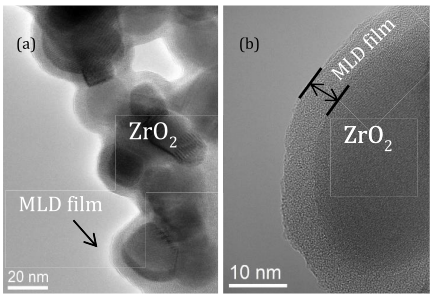

Figure 8. (a) TEM image of ZrO_2 NPs coated with 50 Å thick MLD film deposited using V_4D_4/TMA MLD at 200 °C. (b) Zoom-in image of the same sample.

annealing temperatures. Annealing of the 150 °C-deposited V_4D_4/TMA film at 1100 °C resulted in a 47% decrease in thickness. The same thermal treatment of the 200 °C-deposited V_4D_4/TMA film showed a 28% thickness decrease. The higher decrease observed for the film deposited at 150°C is attributed to its higher carbon content, which is consistent with the XPS observations.

To investigate the dielectric properties of the siloxane-alumina MLD films, the 12 and 40 nm thick V_4D_4-TMA films were tested in a metal/insulator/metal (MIM) device structure (Figure 9c inset). The capacitance per unit area (C_i) vs. frequency (f) and the applied electric field (E_i) are shown in Figure 9a,b, respectively. The siloxane-alumina MLD film resulted in high C_i-s of 150 and 350 nF cm^{-2} for the 40 and 12 nm thick films, respectively, which were stable over a wide range of operating frequencies, that is, 10^3−10^6 Hz. The C_i of the 12 nm thick MLD film showed a slight decrease at frequencies above 600 kHz. This is attributed to the greater polarization effects at the interface between the dielectric and the electrode in the MIM device with thinning down of the films.[8,51] The C_i−E_i graph shows that the C_i values for the V_4D_4-TMA films were constant in the range of ±1.25 MV cm^{-1}, demonstrating the electrical stability of the MLD dielectrics.

From the C_i data, the dielectric constant (k) of the 12 nm thick film was estimated to be 4.7.

The leakage current density curves (J_i vs. E_i) of the 12 and 40 nm thick V_4D_4-TMA films overlapped well (Figure 9c), exhibiting excellent insulating behavior of both MLD films, with J_i values lower than 5.4×10^{-8} A cm^{-2} at −1.25 MV cm^{-1} and 7.6×10^{-9} A cm^{-2} at +1.25 MV cm^{-1}.

The C_i−E_i and J_i−E_i was measured for the 12 nm V_4D_4-TMA film in a wider E_i range of ±2.5 MV cm^{-1} (SI, Figure 3S). The C_i value for the 12 nm film was constant in the range of ±2.5 MV cm^{-1} and the leakage current density was lower than 5.1×10^{-8} A cm^{-2} at ±2.5 MV cm^{-1}.

CONCLUSIONS

In this study, hybrid organic−inorganic siloxane-alumina films were grown by MLD using sequential surface reactions between 1,3,5,7-tetravinyl-1,3,5,7-tetramethylcyclotetrasiloxane (V_4D_4) and trimethylaluminum (TMA) at temperatures between 120 and 200 °C. *In situ* QCM analysis showed a linear mass increase with the number of MLD cycles and revealed self-limiting surface chemistry between TMA and V_4D_4. Infrared spectra of the deposited films showed the strong peak of Si−O−Al at 1015 cm^{-1}, with the shoulder at around 1067 cm^{-1}, attributed to the Si−O−Si bonding. Formation of

https://dx.doi.org/10.1021/acs.chemmater.0c04408
Chem. Mater. XXXX, XXX, XXX−XXX

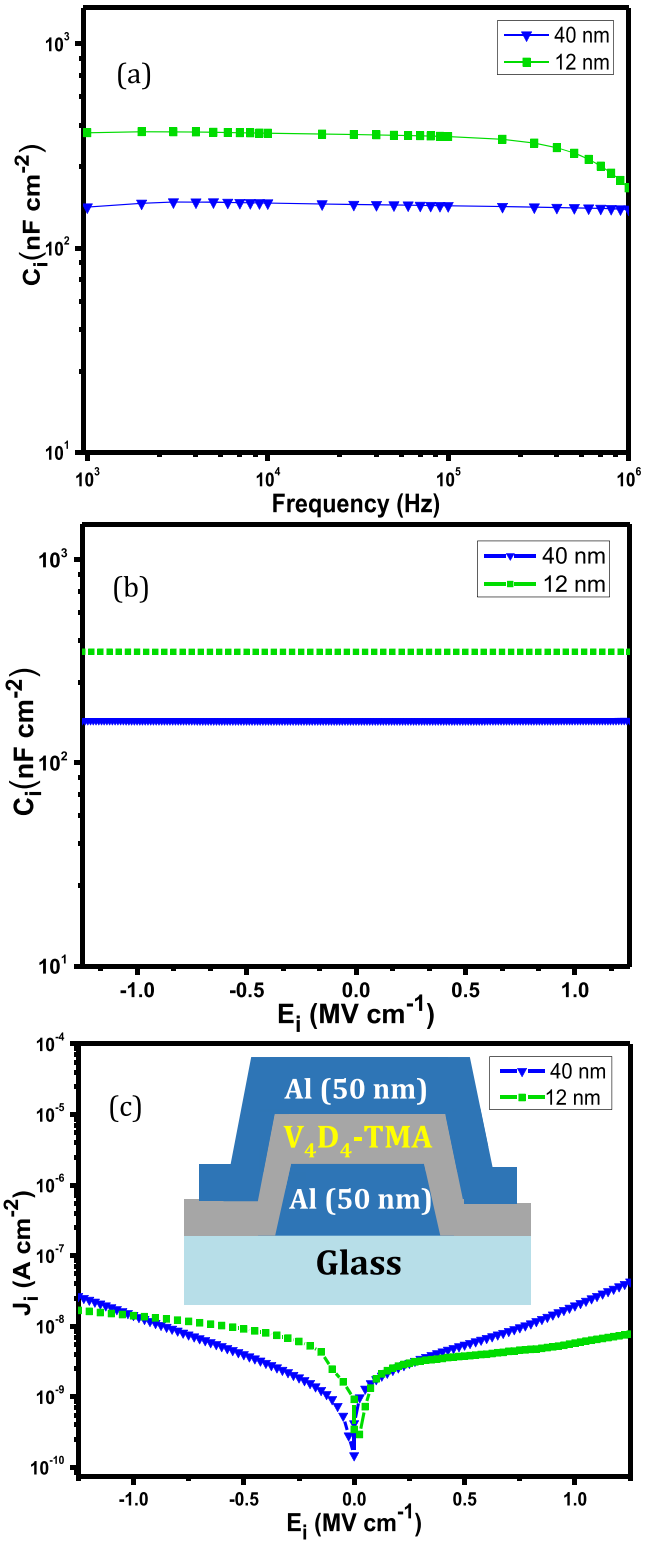

Figure 9. Electrical characteristics of the MLD films: (a) C_i versus frequency; (b) C_i versus E_i; (c) J_i–E_i characteristics of the 40 and 12 nm thick MLD films; (c, inset) structure of the Al/V_4D_4-TMA/Al MIM device used for the characterization; and the C_i versus E_i was measured at 1 kHz with an AC voltage of 10 mV RMS.

Si–O–Al was also confirmed by the XPS analysis, which means that the reaction of V_4D_4 with TMA proceeds through the Si–O–Al bond formation, as we proposed. The FTIR spectra of the film showed a strong peak at 1258 cm^{-1}, suggesting dioxygen-substituted Si atoms. The same degree of oxidation of the silicon atoms in the film was revealed by the XPS. The Si 2p spectral region showed a single peak at 101.9 eV, assigned to the dioxygen-substituted (SiO_2C_2) bonding state of Si within the film, which agrees with the retention of a chain-building SiO_2MeVi unit in V_4D_4. The XPS survey scan showed the ratio of Si to C being 1:3 for all deposition temperatures, which is also consistent with the Si:C ratio in a chain-building SiO_2MeVi unit in V_4D_4. Based on the FTIR and XPS compositional analysis, a realistic V_4D_4/TMA reaction mechanism was suggested, which differs for higher and lower processing temperatures. Consequently, the composition of the films can be tuned with the choice of the deposition temperature. With the V_4D_4-TMA MLD, we attribute the lower than expected Si concentration to the very high reactivity of the TMA molecule, which opens the V_4D_4 ring in more than one region, cleaving it into -O_2SiMeVi units that further react with Al–Me species to form ═Al-O-SiMeVi-O-like structures within the film. TEM showed a highly conformal coating of zirconia nanoparticles by the developed MLD process. The pinhole-free nature and conformal growth inherent to the MLD technique allow the formation of high-quality siloxane-alumina thin films with excellent insulating properties and thermal stability that may have a potential application as ultrathin insulating coatings in modern electronic devices.

■ ASSOCIATED CONTENT

Supporting Information

The Supporting Information is available free of charge at https://pubs.acs.org/doi/10.1021/acs.chemmater.0c04408.

Table 1S summarizes the wavenumbers of the peaks in the ATR-FTIR spectra (Figure 4) and their assignment to the corresponding vibration modes; proposed MLD scheme with diethoxy(methyl)vinylsilane and trimethylaluminum (TMA) as precursors; the thickness changes of the siloxane-alumina films after one-hour annealing in air at various annealing temperatures; the C_i–E_i and J_i–E_i graphs measured for the 12 nm V_4D_4-TMA film in a E_i range of ±2.5 MV cm^{-1} (PDF)

■ AUTHOR INFORMATION

Corresponding Authors

Kristina Ashurbekova – *Dagestan State University, 367000 Makhachkala, Russia;* orcid.org/0000-0001-6647-4872; Email: krashurbekova@inbox.ru

Mato Knez – *CIC nanoGUNE BRTA, E-20018 Donostia-San Sebastián, Spain; IKERBASQUE, Basque Foundation for Science, E-48009 Bilbao, Spain; Department of Physics and Centre for Micro- and Nanosciences and Technologies, University of Rijeka, 51000 Rijeka, Croatia;* orcid.org/0000-0002-9850-1035; Email: m.knez@nanogune.eu

Authors

Karina Ashurbekova – *CIC nanoGUNE BRTA, E-20018 Donostia-San Sebastián, Spain*

Iva Saric – *Department of Physics and Centre for Micro- and Nanosciences and Technologies, University of Rijeka, 51000 Rijeka, Croatia*

Marco Gobbi – *CIC nanoGUNE BRTA, E-20018 Donostia-San Sebastián, Spain; IKERBASQUE, Basque Foundation for Science, E-48009 Bilbao, Spain*

https://dx.doi.org/10.1021/acs.chemmater.0c04408
Chem. Mater. XXXX, XXX, XXX–XXX

Evgeny Modin − *CIC nanoGUNE BRTA, E-20018 Donostia-San Sebastián, Spain;* orcid.org/0000-0002-7403-7610
Andrey Chuvilin − *CIC nanoGUNE BRTA, E-20018 Donostia-San Sebastián, Spain; IKERBASQUE, Basque Foundation for Science, E-48009 Bilbao, Spain*
Mladen Petravic − *Department of Physics and Centre for Micro- and Nanosciences and Technologies, University of Rijeka, 51000 Rijeka, Croatia;* orcid.org/0000-0002-3495-9899
Ilmutdin Abdulagatov − *Dagestan State University, 367000 Makhachkala, Russia;* orcid.org/0000-0002-6299-5280

Complete contact information is available at: https://pubs.acs.org/10.1021/acs.chemmater.0c04408

Author Contributions

The manuscript was written through contributions of all authors. All authors have given approval to the final version of the manuscript.

Notes

The authors declare no competing financial interest.

■ ACKNOWLEDGMENTS

Kr. A. thanks Dr. Aziz Abdulagatov for scientific discussions, feedback, and comments. M.K. is grateful for funding from the Spanish Ministry of Science and Innovation (MICINN) [Grant Agreement No. PID2019-111065RB-I00], including FEDER funds, and the Maria de Maeztu Units of Excellence Programme [grant number MDM-2016-0618]. Ka.A. acknowledges funding through European Union's Horizon 2020 research and innovation program under the Marie Sklodowska-Curie grant agreement No. 765378. I.A. and Kr.A acknowledge funding through the Russian Federation government under the grant number FZNZ-2020-0002. I.S. and M.P. acknowledge support from the University of Rijeka under project number 18−144.

■ REFERENCES

(1) Takano, N.; Fukuda, T.; Ono, K. Analysis of Structures of Oligomeric Siloxanes from Dimethoxydimethylsilane under Heat Treatment by FT-IR. *Polym. J.* **2001**, *33*, 469−474.
(2) Zhou, H.; Bent, S. F. Highly Stable Ultrathin Carbosiloxane Films by Molecular Layer Deposition. *J. Phys. Chem. C* **2013**, *117*, 19967−19973.
(3) Closser, R. G.; Bergsman, D. S.; Bent, S. F. Molecular Layer Deposition of a Highly Stable Silicon Oxycarbide Thin Film Using an Organic Chlorosilane and Water. *ACS Appl. Mater. Interfaces* **2018**, *10*, 24266−24274.
(4) Saed, M. O.; Terentjev, E. M. Siloxane crosslinks with dynamic bond exchange enable shape programming in liquid-crystalline elastomers. *Sci. Rep.* **2020**, *10*, No. 6609.
(5) Kulyk, K.; Zettergren, H.; Gatchell, M.; Alexander, J. D.; Borysenko, M.; Palianytsia, B.; Larsson, M.; Kulik, T. Dimethylsilanone Generation from Pyrolysis of Polysiloxanes Filled with Nanosized Silica and Ceria/Silica. *ChemPlusChem* **2016**, *81*, 1003−1013.
(6) Wallin, T. J.; Pikul, J.; Shepherd, R. F. 3D printing of soft robotic systems. *Nat. Rev. Mater.* **2018**, *3*, 84−100.
(7) Moon, H.; Seong, H.; Shin, W. C.; Park, W.-T.; Kim, M.; Lee, S.; Bong, J. H.; Noh, Y.-Y.; Cho, B. J.; Yoo, S.; Im, S. G. Synthesis of ultrathin polymer insulating layers by initiated chemical vapour deposition for low-power soft electronics. *Nat. Mater.* **2015**, *14*, 628.
(8) Pak, K.; Seong, H.; Choi, J.; Hwang, W. S.; Im, S. G. Synthesis of Ultrathin, Homogeneous Copolymer Dielectrics to Control the Threshold Voltage of Organic Thin-Film Transistors. *Adv. Funct. Mater.* **2016**, *26*, 6574−6582.
(9) Jiang, Y.-B.; Liu, N.; Gerung, H.; Cecchi, J. L.; Brinker, C. J. Nanometer-Thick Conformal Pore Sealing of Self-Assembled Mesoporous Silica by Plasma-Assisted Atomic Layer Deposition. *J. Am. Chem. Soc.* **2006**, *128*, 11018−11019.
(10) Kim, B. J.; Seong, H.; Shim, H.; Lee, Y. I.; Im, S. G. Initiated Chemical Vapor Deposition of Polymer Films at High Process Temperature for the Fabrication of Organic/Inorganic Multilayer Thin Film Encapsulation. *Adv. Eng. Mater.* **2017**, *19*, No. 1600870.
(11) Gleason, K. K.; Yang, R. Antifouling and Chlorine-Resistant Ultrathin Coatings on Reverse Osmosis Membranes. US Patent US2014/0299538A12014.
(12) Lee, J.; Ha, J.-H.; Song, I.-H. Improving the antifouling properties of ceramic membranes via chemical grafting of organosilanes. *Sep. Sci. Technol.* **2016**, *51*, 2420−2428.
(13) O'Shaughnessy, W. S.; Gao, M.; Gleason, K. K. Initiated Chemical Vapor Deposition of Trivinyltrimethylcyclotrisiloxane for Biomaterial Coatings. *Langmuir* **2006**, *22*, 7021−7026.
(14) O'Shaughnessy, W. S.; Murthy, S. K.; Edell, D. J.; Gleason, K. K. Stable Biopassive Insulation Synthesized by Initiated Chemical Vapor Deposition of Poly(1,3,5-trivinyltrimethylcyclotrisiloxane). *Biomacromolecules* **2007**, *8*, 2564−2570.
(15) Achyuta, A.; S Polikov, V.; White, A.; Pryce Lewis, H.; K Murthy, S. Biocompatibility Assessment of Insulating Silicone Polymer Coatings Using an in vitro Glial Scar Assay. *Macromol. Biosci.* **2010**, *10*, 872−80.
(16) Coclite, A. M.; Gleason, K. K. Global and local planarization of surface roughness by chemical vapor deposition of organosilicon polymer for barrier applications. *J. Appl. Phys.* **2012**, *111*, No. 073516.
(17) Hoffmann, J.; Gamboa, S. M.; Hofmann, A.; Gliemann, H.; Welle, A.; Wacker, I.; Schröder, R. R.; Ness, L.; Hagenmeyer, V.; Gengenbach, U. Siloxane-functionalised surface patterns as templates for the ordered deposition of thin lamellar objects. *Sci. Rep.* **2019**, *9*, No. 17952.
(18) Colombo, P.; Mera, G.; Riedel, R.; Sorarù, G. D. Polymer-Derived Ceramics: 40 Years of Research and Innovation in Advanced Ceramics. *J. Am. Ceram. Soc.* **2010**, *93*, 1805−1837.
(19) Barroso, G.; Li, Q.; Bordia, R. K.; Motz, G. Polymeric and ceramic silicon-based coatings − a review. *J. Mater. Chem. A* **2019**, *7*, 1936−1963.
(20) Alvi, S. A.; Akhtar, F. High temperature tribology of polymer derived ceramic composite coatings. *Scientific Reports* **2018**, *8*, 15105.
(21) Baker, C. C.; Chromik, R. R.; Wahl, K. J.; Hu, J. J.; Voevodin, A. A. Preparation of chameleon coatings for space and ambient environments. *Thin Solid Films* **2007**, *515*, 6737−6743.
(22) Erdemir, A. Review of engineered tribological interfaces for improved boundary lubrication. *Tribol. Int.* **2005**, *38*, 249−256.
(23) Tung, S. C.; McMillan, M. L. Automotive tribology overview of current advances and challenges for the future. *Tribol. Int.* **2004**, *37*, 517−536.
(24) George, S. M.; Yoon, B.; Dameron, A. A. Surface Chemistry for Molecular Layer Deposition of Organic and Hybrid Organic−Inorganic Polymers. *Acc. Chem. Res.* **2009**, *42*, 498−508.
(25) Ashurbekova, K.; Ashurbekova, K.; Botta, G.; Yurkevich, O.; Knez, M. Vapor phase processing: a novel approach for fabricating functional hybrid materials. *Nanotechnology* **2020**, *31*, No. 342001.
(26) Malygin, A. A.; Drozd, V. E.; Malkov, A. A.; Smirnov, V. M. From V.B. Aleskovskii's "Framework" Hypothesis to the Method of Molecular Layering/Atomic Layer Deposition. *Chem. Vap. Deposition* **2015**, *21*, 216−240.
(27) Parsons, G. N.; George, S. M.; Knez, M. Progress and future directions for atomic layer deposition and ALD-based chemistry. *MRS Bull.* **2011**, *36*, 865−871.
(28) Abdulagatov, A. I.; Terauds, K. E.; Travis, J. J.; Cavanagh, A. S.; Raj, R.; George, S. M. Pyrolysis of Titanicone Molecular Layer Deposition Films as Precursors for Conducting TiO2/Carbon Composite Films. *J. Phys. Chem. C* **2013**, *117*, 17442−17450.
(29) Burton, B. B.; Kang, S. W.; Rhee, S. W.; George, S. M. SiO2 Atomic Layer Deposition Using Tris(dimethylamino)silane and

Hydrogen Peroxide Studied by in Situ Transmission FTIR Spectroscopy. *J. Phys. Chem. C* **2009**, *113*, 8249−8257.
(30) KLAUS, J. W.; SNEH, O.; OTT, A. W.; GEORGE, S. M. ATOMIC LAYER DEPOSITION OF SiO2 USING CATALYZED AND UNCATALYZED SELF-LIMITING SURFACE REACTIONS. *Surf. Rev. Lett.* **1999**, *06*, 435−448.
(31) Klaus, J. W.; George, S. M. Atomic layer deposition of SiO2 at room temperature using NH3-catalyzed sequential surface reactions. *Surf. Sci.* **2000**, *447*, 81−90.
(32) Klaus, J. W.; Sneh, O.; George, S. M. Growth of SiO2 at Room Temperature with the Use of Catalyzed Sequential Half-Reactions. *Science* **1997**, *278*, 1934−1936.
(33) Ferguson, J. D.; Smith, E. R.; Weimer, A. W.; George, S. M. ALD of SiO2 at Room Temperature Using TEOS and H2O with NH3 as the Catalyst. *J. Electrochem. Soc.* **2004**, *151*, G528−G535.
(34) Abdulagatov, A. I. Growth, Characterization and Post-processing of Inorganic and Hybrid Organic-inorganic Thin Films Deposited using Atomic and Molecular Layer Deposition Techniques. Ph.D. Thesis University of Colorado at Boulder, 2012.
(35) George, S. M.; Yoon, B.; Hall, R. A.; Abdulagatov, A. I.; Gibbs, Z. M.; Lee, Y.; Seghete, D.; Lee, B. H. Molecular Layer Deposition of Hybrid Organic−Inorganic Films. In *Atomic Layer Deposition of Nanostructured Materials* (eds Pinna, N.; Knez, M., Eds.; Wiley: 2012; pp 83−107.
(36) Ashurbekova, K.; Ashurbekova, K.; Saric, I.; Modin, E.; Petravić, M.; Abdulagatov, I.; Abdulagatov, A.; Knez, M. Molecular layer deposition of hybrid siloxane thin films by ring opening of cyclic trisiloxane (V3D3) and azasilane. *Chem. Commun.* **2020**, *56*, 8778−8781.
(37) Huang, Z. Combining Ar ion milling with FIB lift-out techniques to prepare high quality site-specific TEM samples. *J. Microsc.* **2004**, *215*, 219−223.
(38) Jones, R. G.; Ando, W.; Chojnowski, J. *Silicon-Containing Polymers. The Science and Technology of their Synthesis and Applications*; Springer Science+Business Media: Dordrecht, 2000; Vol. *763*, 17.
(39) Dubois, Philippe.; Coulembier, Olivier.; Raquez, J.-M.. *Handbook of Ring-Opening Polymerization*; WILEY-VCH Verlag GmbH & Co. KGaA: Weinheim, 2009; *425*, 50.
(40) Zhou, H.; Bent, S. F. Fabrication of organic interfacial layers by molecular layer deposition: Present status and future opportunities. *J. Vac. Sci. Technol. A* **2013**, *31*, No. 040801.
(41) Groner, M.; Fabreguette, F.; Elam, J.; George, S. M. Low-Temperature Al2O3 Atomic Layer Deposition. *Chem. Mater.* **2004**, *16*, 639−645.
(42) Qiu, H.; Hölken, I.; Gapeeva, A.; Filiz, V.; Adelung, R.; Baum, M. Development and Characterization of Mechanically Durable Silicone-Polythiourethane Composites Modified with Tetrapodal Shaped ZnO Particles for the Potential Application as Fouling-Release Coating in the Marine Sector. *Materials* **2018**, 2413.
(43) Burkey, D.; Gleason, K. Temperature-resolved Fourier transform infrared study of condensation reactions and porogen decomposition in hybrid organosilicon-porogen films. *J. Vac. Sci. Technol. A* **2004**, *22*, 61−70.
(44) Hesse, R.; Chassé, T.; Szargan, R. Peak shape analysis of core level photoelectron spectra using UNIFIT for WINDOWS. *Fresenius' J. Anal. Chem.* **1999**, *365*, 48−54.
(45) O'Hare, L.-A.; Hynes, A.; Alexander, M. R. A methodology for curve-fitting of the XPS Si 2p core level from thin siloxane coatings. *Surf. Interface Anal.* **2007**, *39*, 926−936.
(46) Kloprogge, J. T.; Duong, L.; Wood, B.; Frost, R. XPS study of the major minerals in bauxite: Gibbsite, bayerite and (pseudo-)boehmite. *J. Colloid Interface Sci.* **2006**, *296*, 572−6.
(47) Che, J.; Xiao, Y.; Wang, X.; Pan, A.; Yuan, W.; Wu, X. Grafting polymerization of polyacetal onto nano-silica surface via bridging isocyanate. *Surf. Coat. Technol.* **2007**, 4578−84.
(48) Herreros, B.; He, H.; Barr, T. L.; Klinowski, J. ESCA Studies of Framework Silicates with the Sodalite Structure: 1. Comparison of Purely Siliceous Sodalite and Aluminosilicate Sodalite. *J. Phys. Chem. A* **1994**, *98*, 1302−1305.
(49) Chen, L.; Ye, G.; Li, K.; Wang, Q.; Xu, D.; Guo, M. Al-O-Si Bond Formation in Boehmite-Fumed Silica Mixtures during Mechanochemical Activation. *Interceram* **2014**, *63*, 372−375.
(50) Anderson, P. R.; Swartz, W. E. X-ray photoelectron spectroscopy of some aluminosilicates. *Inorg. Chem.* **1974**, *13*, 2293−2294.
(51) Ku, C. C.; Liepins, R. *Electrical Properties of Polymers: Chemical Principles*; Hanser Publishers: Munich, Vienna, New York, 1987; Vol. *389*, pp 165.

https://dx.doi.org/10.1021/acs.chemmater.0c04408
Chem. Mater. XXXX, XXX, XXX−XXX